

## Poly(ADP-ribose) Polymerase Null Mouse Cells Synthesize ADP-ribose Polymers\*

(Received for publication, August 21, 1998)

W. Melissa Shieh‡, Jean-Christophe Amé§, Mandala V. Wilson‡, Zhao-Qi Wang¶, David W. Koh§, Myron K. Jacobson§\*\*, and Elaine L. Jacobson‡\*\*\*

From the ‡Department of Clinical Sciences, §Lucille P. Markey Cancer Center, §College of Pharmacy, and \*\*Advanced Science and Technology Commercialization Center, University of Kentucky, Lexington, Kentucky 40506-0286 and ¶International Agency for Research on Cancer (IARC), Unit of Gene Environment Interaction, IARC, 150, cours Albert-Thomas, F-69372 Cedex 08, Lyon, France

Poly(ADP-ribose) polymerase (PARP) (EC 2.4.2.30), the only enzyme known to synthesize ADP-ribose polymers from NAD<sup>+</sup>, is activated in response to DNA strand breaks and functions in the maintenance of genomic integrity. Mice homozygous for a disrupted gene encoding PARP are viable but have severe sensitivity to  $\gamma$ -radiation and alkylating agents. We demonstrate here that both 3T3 and primary embryo cells derived from PARP<sup>-/-</sup> mice synthesized ADP-ribose polymers following treatment with the DNA-damaging agent, *N*-methyl-*N'*-nitro-*N*-nitrosoguanidine, despite the fact that no PARP protein was detected in these cells. ADP-ribose polymers isolated from PARP<sup>-/-</sup> cells were indistinguishable from that of PARP<sup>+/+</sup> cells by several criteria. First, they bound to a boronate resin selective for ADP-ribose polymers. Second, treatment of polymers with snake venom phosphodiesterase and alkaline phosphatase yielded ribosyladenosine, a nucleoside diagnostic for the unique ribosyl-ribosyl linkages of ADP-ribose polymers. Third, they were digested by treatment with recombinant poly(ADP-ribose) glycohydrolase, an enzyme highly specific for ADP-ribose polymers. Collectively, these data demonstrate that ADP-ribose polymers are formed in PARP<sup>-/-</sup> cells in a DNA damage-dependent manner. Because the PARP gene has been disrupted, these results suggest the presence of a previously unreported activity capable of synthesizing ADP-ribose polymers in PARP<sup>-/-</sup> cells.

Poly(ADP-ribose) polymerase (PARP)<sup>1</sup> (EC 2.4.2.30) is a nu-

\* This work was supported in part by National Institutes of Health Grants CA65579 and CA43894. The costs of publication of this article were defrayed in part by the payment of page charges. This article must therefore be hereby marked "advertisement" in accordance with 18 U.S.C. Section 1734 solely to indicate this fact.

‡ To whom correspondence should be addressed: A323A ASTeCC Bldg., University of Kentucky, Lexington, KY 40506-0286. Tel.: 606-257-2300 (ext. 235); Fax: 606-257-2489; E-mail: ejacob@pop.uky.edu.

<sup>1</sup> The abbreviations used are: PARP, poly(ADP-ribose) polymerase; kb, kilobase pair; PBS, phosphate-buffered saline; SSPE, saline/sodium phosphate/EDTA buffer; PAGE, polyacrylamide gel electrophoresis; rAdo, ribosyladenosine; MOPS, 3-(*N*-morpholino)propanesulfonic acid; HPLC, high pressure liquid chromatography; MNNG, *N*-methyl-*N'*-nitro-*N*-nitrosoguanidine; PARP, poly(ADP-ribose) glycohydrolase.

clear enzyme that catalyzes the formation of complex homopolymers of ADP-ribose from NAD<sup>+</sup> on nuclear proteins in response to DNA damage. Recently, mice homozygous for a disrupted PARP gene (PARP<sup>-/-</sup>) have been generated (1–3). These animals and cells derived from them are being widely studied to better understand the potential roles of ADP-ribose polymer metabolism in cellular functions including DNA repair (4) and apoptosis (5, 6). The PARP<sup>-/-</sup> mice show normal fetal and postnatal development (1, 2) but have inherent genomic instability and are highly sensitive to DNA damage induced by  $\gamma$ -radiation and alkylating agents (2, 4, 5). These results indicate that PARP is involved in maintaining genomic integrity and cell survival, especially following genotoxic insults. However, viability of the null genotype mice suggests that PARP is not essential for growth, development, or differentiation. Because there has been only a single gene product reported with PARP activity, we have used the PARP null genotype to address whether any other activities might be present that are capable of generating ADP-ribose polymers. Here, we show that cells derived from PARP<sup>-/-</sup> animals form ADP-ribose polymers, indicating the presence of enzymatic activity capable of catalyzing ADP-ribose polymer synthesis, which may represent heretofore unreported family member(s) of PARP.

### EXPERIMENTAL PROCEDURES

**Cell Culture**—PARP<sup>+/+</sup> and PARP<sup>-/-</sup> mice (strain C57BL/6) developed by Wang *et al.* (1) were used for the studies described here. Primary mouse embryo or immortalized 3T3 (PARP<sup>+/+</sup> clone A19, PARP<sup>-/-</sup> clone A4, and PARP<sup>-/-</sup> clone A1) cells were grown in Dulbecco's modified Eagle's medium supplemented with 10% bovine calf serum (Hyclone).

**Southern Blot Analyses**—Total genomic DNA from cultured cells of different PARP genetic backgrounds (+/+, +/-, and -/-) was prepared as described previously (7). DNA (10  $\mu$ g) was digested with *Pvu*II, fractionated on a 1% agarose gel, transferred to a nylon membrane (Hybond N+, Amersham Pharmacia Biotech), and hybridized to a PARP gene-specific probe (1), a 0.5-kb *Xho*I-*Hind*III fragment <sup>32</sup>P-radiolabeled (3.2  $\times$  10<sup>6</sup> dpm/ng of DNA) by a random hexamer priming method (8). Prehybridization and hybridization were carried out at 42 °C in 50% formamide, containing 0.25 M sodium phosphate buffer, pH 7.2, 0.25 M NaCl, 3% SDS, 1 mM EDTA, 5 $\times$  Denhardt's solution (7), and 10% (w/v) dextran sulfate. After extensive washing in 2 $\times$  SSPE and in 0.2 $\times$  SSPE containing 1% SDS at 65 °C, blots were subjected to autoradiography at -80 °C for 6 h using Kodak Biomax MS film and intensifying screens.

**Western Blot Analyses**—Cells were collected by centrifugation following removal from culture dishes with trypsin and dissolved in PBS containing 0.5% sodium deoxycholate, 0.1% SDS, 1% Triton X-100, 0.5% Nonidet P-40, 5 mM EDTA, and freshly prepared protease inhibitors, 1 mM phenylmethylsulfonyl fluoride, 0.001% aprotinin, 0.001% leupeptin. Proteins were quantified by the method of Bradford (9). Following sonification for 30 s at 35% power, the proteins were separated by SDS-PAGE on a 10% gel and transferred to nitrocellulose membranes (0.2  $\mu$ m, Optitrans from Schleicher & Schuell) for Western blot analyses. The blots were blocked in TBS-Tween (50 mM Tris-HCl, pH 8.0, 150 mM NaCl, 0.05% Tween 20 (v/v)) containing 5% fat-free dry milk and incubated with PARP antibody at 1:1333 dilution (A252, Biomol, Plymouth, PA) that was an antipeptide antibody generated against the carboxyl-terminal portion of the automodification domain of PARP. Immunoreactive material was revealed by incubating with secondary anti-rabbit IgG-peroxidase (A-545, Sigma) at 1:30,000 dilution in TBS-Tween containing 5% fat-free dry milk. The Amersham ECL system was used for detection.

**Measurement of NAD<sup>+</sup>**—Intracellular NAD<sup>+</sup> was extracted from cells in midexponential phase of growth. Cell numbers were similar for PARP<sup>+/+</sup> and PARP<sup>-/-</sup> cells within a given experiment. MNNG was prepared freshly in Me<sub>2</sub>SO so that the final concentration of the solvent

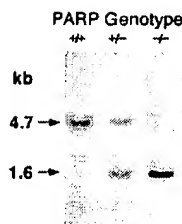


FIG. 1. Southern blot analyses of 3T3 cells from mice of various PARP genotypes. DNA was isolated from cultured cells derived from mice of various PARP genotypes and digested with *PvuII*, separated by agarose gel electrophoresis, transferred to a nylon membrane, and probed with a PARP-specific probe (1).

was 0.5% (v/v) when added to the culture medium. Following a 20-min treatment period, the medium was removed, and the cells were washed twice with PBS. The cells were extracted using 0.5 M  $\text{HClO}_4$  at 4 °C. The acid-insoluble material was removed by centrifugation, and the resulting supernatant fraction was adjusted to pH 7.3 with 1.0 M KOH, 0.33 M potassium phosphate. Following removal of the potassium perchlorate precipitate,  $\text{NAD}^+$  was determined by an enzymic cycling assay as described previously (10).

**Measurement of Poly(ADP-ribose) Accumulation**—For quantification of ADP-ribose polymers, cells were grown to confluence and incubated with [ $^3\text{H}$ ]adenine for 16 h to radiolabel the  $\text{NAD}^+$  pool. To induce ADP-ribose polymer synthesis, cells were incubated in 136  $\mu\text{M}$  MNNG at 37 °C for 20 min, followed by addition of 20% (w/v) trichloroacetic acid at 4 °C. The trichloroacetic acid-insoluble material was collected by centrifugation and applied to a dihydroxyboronyl-Bio-Rex column as described previously (11). The eluate containing ADP-ribose polymers was lyophilized to dryness and resuspended in 2 ml of 50 mM MOPS buffer, 5 mM  $\text{MgCl}_2$ , pH 7.5. The sample was digested with 1 unit of snake venom phosphodiesterase (Worthington) and 1 unit of alkaline phosphatase (Sigma) at 37 °C for 3 h. The digestion mixture was passed through a 0.45- $\mu\text{m}$  filter and analyzed by HPLC on a 5- $\mu\text{m}$  Beckman C18 ODS-reversed phase column (4.6 mm  $\times$  25 cm) using 7 mM ammonium formate, 7% methanol as the running solvent at a flow rate of 1 ml/min. Standards of adenosine and deoxyadenosine, 10 nmol each, were coinjected with each sample.

## RESULTS

**Analysis of PARP Genotype in Cultured Cells**—Fig. 1 shows Southern blot analyses of total genomic DNA isolated from 3T3 cells derived from embryos of various PARP genotypes as revealed by hybridization with a previously described probe (1). Digestion of genomic DNA with *PvuII* generated a 4.7-kb DNA fragment in the  $\text{PARP}^{+/+}$  genotype, a 1.7-kb DNA fragment in the  $\text{PARP}^{-/-}$  genotype, and both fragments in the  $\text{PARP}^{+/-}$  genotype. The same results were observed when genomic DNA was isolated from primary mouse embryo cells obtained from the respective genotypes (data not shown).

**Detection of PARP Protein by Western Blot Analyses**—We examined for the presence of PARP protein in cultured mouse cells of various PARP genotypes using an antipeptide antibody developed against the carboxyl-terminal region of the auto-modification domain of PARP. A SDS-PAGE gel was loaded with a total of 30  $\mu\text{g}$  of protein from 3T3 cell extracts and 60  $\mu\text{g}$  of protein from primary embryo fibroblasts. The only detectable differences between the various genotypes were in the region expected for full-length PARP as shown in Fig. 2. For 3T3 cells, a band of immunoreactive material at approximately 116 kDa was observed in  $\text{PARP}^{+/+}$  cells, whereas a band of less intensity was observed in  $\text{PARP}^{+/-}$  cells, and no band was detectable in the PARP null genotype. Likewise, extracts of primary embryo cells from  $\text{PARP}^{+/+}$  mice showed an intense band at 116 kDa whereas no PARP protein was detected in analyses of extracts of cells from  $\text{PARP}^{-/-}$  animals (Fig. 2).

**MNNG-induced  $\text{NAD}^+$  Consumption**—The activation of PARP by treatment of cells with alkylating agents is known to lead to a rapid consumption of the cellular  $\text{NAD}^+$  pool (12, 13). We studied the effect of a 20-min treatment of MNNG on the

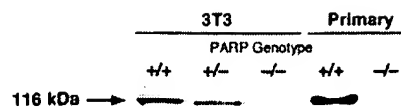


FIG. 2. Western blot analyses of cell extracts for PARP. Total cell protein was separated by SDS-PAGE, transferred to a nitrocellulose membrane, and probed with a PARP antibody. Immunoreactive material was detected as described under "Experimental Procedures."

$\text{NAD}^+$  content of 3T3 and primary embryo cells from the different PARP genotypes. Fig. 3 shows the  $\text{NAD}^+$  content of 3T3 cells of different PARP genotypes as a function of time following treatment with 68  $\mu\text{M}$  MNNG (Fig. 3B) and as a function of MNNG dose 240 min following treatment (Fig. 3A). The data are presented as percent of control  $\text{NAD}^+$  content because of a slightly different number of cells and initial  $\text{NAD}^+$  content for the two genotypes ( $1.5 \times 10^5$  for  $\text{PARP}^{+/+}$  versus  $2.2 \times 10^5$  for  $\text{PARP}^{-/-}$  cells). Initial  $\text{NAD}^+$  values were 120 and 140 pmol/sample, respectively. Both  $\text{PARP}^{+/+}$  and  $\text{PARP}^{-/-}$  cells showed time- and dose-dependent depletion of  $\text{NAD}^+$ , although depletion appeared to be slightly slower in the  $\text{PARP}^{-/-}$  cells. When 500  $\mu\text{M}$  benzamide, a known inhibitor of ADP-ribosyltransferases, was added to the culture medium, rates of  $\text{NAD}^+$  consumption were suppressed in cells from both genotypes. Results similar to those shown in Fig. 3 were obtained with primary embryo cells from  $\text{PARP}^{+/+}$  and  $\text{PARP}^{-/-}$  mice (data not shown).

**ADP-ribose Polymer Accumulation in MNNG-treated Cells**—Because we observed depletion of  $\text{NAD}^+$  following treatment of  $\text{PARP}^{-/-}$  cells with MNNG, we investigated the possibility that these cells contain an activity capable of catalyzing conversion of  $\text{NAD}^+$  to ADP-ribose polymers. Both  $\text{PARP}^{+/+}$  and  $\text{PARP}^{-/-}$  3T3 cells were radiolabeled with [ $^3\text{H}$ ]adenine and examined for the presence of ADP-ribose polymers using a method previously described (11). In this method, ADP-ribose polymers are isolated using a boronyl resin and digested with snake venom phosphodiesterase and alkaline phosphatase, which results in the generation of ribosyladenosine (rAdo), a nucleoside unique to the ribosyl-ribosyl linkages of ADP-ribose polymers (14). The presence of radiolabeled rAdo (formed from internal polymer residues) and Ado (formed from terminal residues) was then examined by HPLC as shown in Fig. 4. Although radiolabeled Ado can result from either ADP-ribose polymers or from RNA, rAdo is diagnostic for ADP-ribose polymers (14). In the absence of MNNG treatment, no detectable rAdo was present in either the  $\text{PARP}^{+/+}$  or  $\text{PARP}^{-/-}$  cells (Fig. 4, A and B), although small amounts of Ado were detected, most likely from a small contamination with RNA. Following treatment with 136  $\mu\text{M}$  MNNG for 20 min, radiolabel co-eluting with rAdo was demonstrated in both genotypes (Fig. 4, C and D), although the amount present in the  $\text{PARP}^{-/-}$  cells was less. Quantification is shown in Table I below from an experiment in which the specific radioactivity of the  $\text{NAD}^+$  pool in each cell type was measured. Average polymer size, estimated by the relative amounts of rAdo and Ado, was approximately 3.4 residues in  $\text{PARP}^{+/+}$  cells and 1.7 residues in  $\text{PARP}^{-/-}$  cells. When the ADP-ribosyltransferase inhibitor benzamide was present during the MNNG treatment, rAdo accumulation was suppressed by more than 80% in both PARP genotypes (Fig. 4, E and F). The presence of radiolabel co-eluting with rAdo indicates that  $\text{PARP}^{-/-}$  cells retain the ability, albeit reduced, to generate ADP-ribose polymers following DNA damage. Two additional experiments were done to determine whether the radiolabel eluting at the position of rAdo was derived from ADP-ribose polymers. First, when phosphodiesterase and alkaline phosphatase were omitted from the analyses, no radiolabel migrated at the position of rAdo for either  $\text{PARP}^{+/+}$  or  $\text{PARP}^{-/-}$

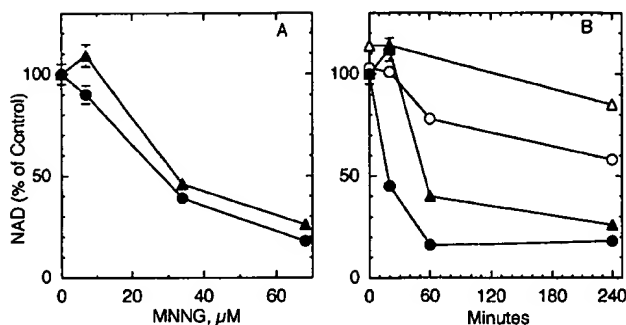


FIG. 3. Effect of MNNG treatment on the NAD<sup>+</sup> content of 3T3 cells derived from PARP<sup>+/+</sup> and PARP<sup>-/-</sup> mice. Cells in exponential growth were treated with MNNG as described under "Experimental Procedures." A, NAD<sup>+</sup> content at 240 min following a 20-min treatment with different doses of MNNG. B, time course of NAD<sup>+</sup> consumption following a 20-min treatment with 68  $\mu\text{M}$  MNNG. Triangles represent PARP<sup>-/-</sup> cells, and circles represent PARP<sup>+/+</sup> cells. Open symbols represent cultures containing 500  $\mu\text{M}$  benzamide. Error bars representing standard deviations from triplicate measurements are shown for values larger than the size of the symbols. A representative experiment is shown. This experiment was repeated 5 times.

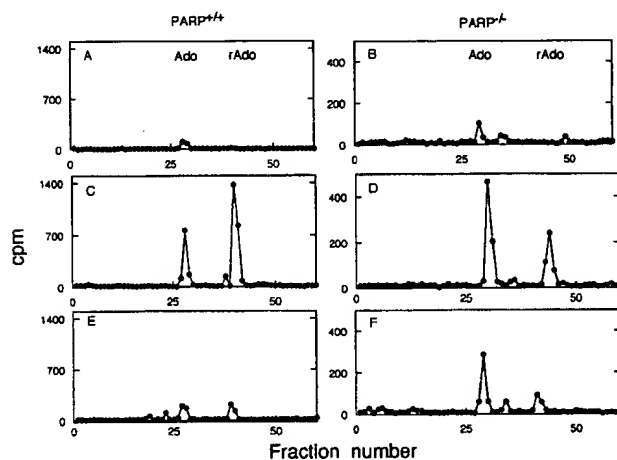


FIG. 4. HPLC analyses of nucleosides obtained from ADP-ribose polymer preparations from 3T3 cells. Confluent 60-mm dishes of cells ( $1.5\text{--}1.8 \times 10^6$  cells) were labeled with 2.5 ml of medium containing 18  $\mu\text{Ci/ml}$  [<sup>3</sup>H]adenine for 16 h. ADP-ribose polymers were isolated and digested as described under "Experimental Procedures." A, C, and E show analyses from PARP<sup>+/+</sup> cells, and B, D, and F show analyses from PARP<sup>-/-</sup> cells. In A and B cells were not treated; in C and D, cells were exposed to 136  $\mu\text{M}$  MNNG for 20 min; in E and F, 1 mM benzamide was present during the MNNG treatment period. Ado and rAdo mark the elution position of the respective nucleosides. Label eluting at approximately 35 min corresponds to deoxyadenosine, representing a small contamination of DNA in polymer preparations from PARP<sup>-/-</sup> cells.

cells (data not shown), demonstrating that the material was derived from polymers sensitive to these enzymes. Second, polymer preparations were treated with purified recombinant poly(ADP-ribose) glycohydrolase (PARG) before digestion with phosphodiesterase and alkaline phosphatase. PARG specifically catalyzes hydrolysis of the ribosyl-ribosyl linkages in ADP-ribose polymer residues forming ADP-ribose (15); thus, PARG treatment should result in the loss of rAdo and the formation of Ado when ADP-ribose polymers treated with PARG are subsequently treated with phosphodiesterase and alkaline phosphatase. The data of Fig. 5 compare the results obtained with and without PARG digestion of polymers isolated from MNNG-treated PARP<sup>-/-</sup> 3T3 cells. All of the radiolabel co-eluting with rAdo was converted to Ado when polymers were treated with PARG before digestion to nucleosides, demon-

TABLE I

## Quantification of ADP-ribose polymers in MNNG-treated cells

Cells were treated with 136  $\mu\text{M}$  MNNG, and ADP-ribose polymers were isolated and quantified as described (11). Benzamide concentration was 1 mM. The data shown are from a representative experiment. Each analysis was conducted at least 3 times. ND means not determined.

Cell type	MNNG	MNNG + benzamide	MNNG + PARG <sup>a</sup>
		pmol rAdo/ $10^6$ cells	
3T3 PARP <sup>+/+</sup>	9.3	1.4	ND
3T3 PARP <sup>-/-</sup>	2.3	0.4	<0.1
PARP <sup>+/+</sup> primary cells	10.8	1.1	ND
PARP <sup>-/-</sup> primary cells	0.3	<0.1	<0.1

<sup>a</sup> ADP-ribose polymers were treated with PARG before digestion to nucleosides.

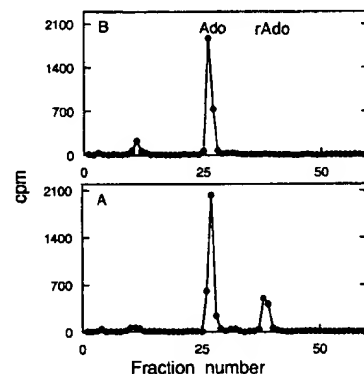


FIG. 5. Effect of PARG treatment on ADP-ribose polymer preparations from PARP<sup>-/-</sup> 3T3 cells. Confluent 100-mm dishes of PARP<sup>-/-</sup> cells ( $3.8 \times 10^6$ ) were labeled with 7.5 ml of medium containing 45  $\mu\text{Ci/ml}$  [<sup>3</sup>H]adenine for 16 h. The cells were treated with MNNG, and ADP-ribose polymers were isolated as described under "Experimental Procedures." A shows the HPLC analysis of nucleosides formed when ADP-ribose polymers were treated with snake venom phosphodiesterase and alkaline phosphatase. B shows an analysis of an equal aliquot of polymers that were subjected to treatment with PARG before phosphodiesterase and alkaline phosphatase treatment. The results of a representative experiment are shown.

strating that the polymers synthesized in PARP<sup>-/-</sup> cells serve as a substrate for PARG. The same result was obtained in studies using primary embryo cells from PARP<sup>-/-</sup> mice.

Quantitative comparisons of ADP-ribose polymer accumulation following MNNG treatment in 3T3 and primary embryo cells of various PARP genotypes are shown in Table I. The quantification of ADP-ribose polymer residues was determined by first measuring the specific radioactivity of the NAD<sup>+</sup> pools in each cell type (11), because the different growth rates of the cells result in slightly different specific radioactivities. The amount of polymer accumulated was similar in both primary embryo cells and 3T3 cells from the PARP<sup>+/+</sup> genotype following MNNG treatment. However, the 3T3 PARP<sup>-/-</sup> cells accumulated approximately 25% of that observed in the 3T3 PARP<sup>+/+</sup> cells, whereas in primary cells polymer accumulation was less than 3% in the null genotype compared with wild type cells.

## DISCUSSION

We have demonstrated in cells derived from PARP<sup>-/-</sup> mice activity that forms ADP-ribose polymers in response to DNA damage. The cultures analyzed for NAD<sup>+</sup> and ADP-ribose polymer content were genotyped by Southern analyses to verify disruption of the PARP gene, ruling out the possibility of errors in identification or cross-contamination of cultures. In addition, we have shown by Western blot analyses that there is no detectable expression of full-length PARP protein or cross-reactive material unique to PARP<sup>-/-</sup> cultured cells.

The amount of ADP-ribose polymers accumulated in PARP<sup>-/-</sup> cells following treatment with MNNG was considerably less than that measured in PARP<sup>+/+</sup> cells. This difference was more pronounced in primary embryo cells than in 3T3 cells. The procedure used to derive 3T3 cells requires continuous cell division and may have selected for cells with a greater ability to synthesize ADP-ribose polymers. This may indicate that the ability to generate ADP-ribose polymers provides a selective advantage in growth or it may reflect a decreased expression of this activity in primary embryo cells, which are more highly differentiated than 3T3 cells.

Although the PARP<sup>-/-</sup> cells showed reduced accumulation of ADP-ribose polymers following MNNG treatment, the amount of NAD<sup>+</sup> consumed was quite similar in both genotypes. The inhibitor benzamide suppressed both NAD<sup>+</sup> consumption and polymer accumulation, suggesting that NAD<sup>+</sup> consumption was because of ADP-ribosyltransferase activity. Polymers of ADP-ribose synthesized in response to DNA damage are rapidly turned over (16, 17); thus, NAD<sup>+</sup> consumption reflects total polymer synthesis. Under these rapid turnover conditions, polymer accumulation reflects the relative rates of synthesis and degradation by PARP and PARG, respectively. The amount of NAD<sup>+</sup> consumed in experiments reported here suggests that the total amount of ADP-ribose polymers synthesized in the PARP<sup>-/-</sup> cells is similar to that in the PARP<sup>+/+</sup> cells. Because cells from the PARP<sup>-/-</sup> mice have unaltered PARG activity (18), the net accumulation of ADP-ribose polymers would be expected to be less in PARP<sup>-/-</sup> cells, as was reported here. A decreased ability to generate polymers combined with unaltered PARG activity would also be expected to result in smaller polymer size, which also was observed.

The ADP-ribose polymers synthesized in PARP<sup>-/-</sup> cells were indistinguishable from that of PARP-containing cells as determined by several criteria. Their synthesis was stimulated by DNA damage and inhibited by benzamide, they were precipitated by trichloroacetic acid, they bound to dihydroxyboronyl-Bio-Rex resin, and they were converted to rAdo and Ado following treatment with snake venom phosphodiesterase and alkaline phosphatase. The material characterized in PARP<sup>-/-</sup> cells cannot be derived from protein-bound monomers of ADP-ribose, which would have yielded only Ado using these digestion conditions. Furthermore, the ribosyl-ribosyl linkages of the polymers were digested by PARG, which is highly specific for ADP-ribose polymers. These data support the argument that PARP<sup>-/-</sup> cells are capable of synthesizing ADP-ribose polymers.

Two possible explanations can be offered for the activity responsible for ADP-ribose polymer synthesis in PARP<sup>-/-</sup> cells. First, a fragment of the disrupted PARP gene may be expressed by some unknown mechanism; however, both this study and previous studies have been unable to detect expression of fragments of PARP in cells of the PARP null genotype. Alternatively, other enzymes heretofore undetected may be present as redundant activities for this metabolism. This possibility is supported by the report of nucleotide sequences representing two putative PARP genes in *Zea mays* (GenBank accession nos. AJ222588 and AJ222589) and a recent report of a nucleotide sequence in mice (GenBank accession no. AF072521), with significant homology to the catalytic domain PARP, which may encode a second enzyme with PARP activity. This nucleotide sequence does not contain homologous amino acid sequences to those used to raise the antibodies used in this study to detect PARP. Thus, we would not have detected the expression of this gene product in the experiments reported here. Regardless of the origin of the activity reported here in PARP<sup>-/-</sup> cells, it only partially compensates for PARP depletion. The population dou-

bling time of PARP<sup>-/-</sup> cells was approximately 43 h compared with 20 h for PARP<sup>+/+</sup> cells (data not shown) (5). This extended cell cycle time is likely the result of loss of function for PARP, which is known to interact with DNA polymerase  $\alpha$  during the S and G<sub>2</sub> phases of the cell cycle (19). Further, PARP has been shown to be a component of the multienzyme replication complex (20). It has been hypothesized to function as a component of the DNA damage surveillance network that coordinates cellular responses to DNA damage with the replication apparatus (19). This hypothesis is supported by the observations that PARP<sup>-/-</sup> cells exhibit increased genomic instability, which is increased 4–5-fold by DNA damage. Another defect in PARP<sup>-/-</sup> cells is a decreased rate of base excision repair (4). Recent studies have shown that PARP interacts directly with DNA repair enzymes, such as XRCC1, DNA polymerase  $\beta$ , and ligase III, presumably to recruit and coordinate various components of the base excision repair pathway (4). In PARP<sup>-/-</sup> cells, the lack of PARP and the resulting DNA repair defects appear to be causal for alkylating agent-induced G<sub>2</sub>M cell cycle blocks, chromosome abnormalities, and cytotoxicity (4, 5). Thus, deficiencies in the PARP pathway, either genetic or nutritional (21, 22), appear to have adverse consequences as these deficiencies have been shown to disrupt DNA repair and some apoptotic signaling pathways (6). The activity capable of ADP-ribose polymer synthesis reported here, which is similar to PARP by its sensitivity to benzamide and its activation by DNA damage, does not serve as a complete replacement for PARP, but its presence may indicate that the ability to metabolize poly(ADP-ribose) may be essential for survival and normal development.

#### REFERENCES

- Wang, Z.-Q., Auer, B., Stingl, L., Berghammer, H., Haidacher, D., Schweiger, M., and Wagner, E. F. (1995) *Genes Dev.* **9**, 509–520
- de Murcia, J. M., Niedergang, C., Trucco, C., Ricoul, M., Dutrillaux, B., Mark, M., Oliver, F. J., Masson, M., Dierich, A., LeMour, M., Walzinger, C., Chambon, P., and de Murcia, G. (1997) *Proc. Natl. Acad. Sci. U. S. A.* **94**, 7303–7307
- Masutani, M., Nozaki, T., Nishiyama, E., Tachi, Y., Shimokawa, T., Ochiya, T., Nakagawa, H., Wakabayashi, K., Watanabe, M., Suzuki, H., and Sugimura, T. (1998) *Proc. Am. Assoc. Cancer Res.* **39**, 473
- Trucco, C., Oliver, F. J., de Murcia, G., and Menissier-de Murcia, J. (1998) *Nucleic Acids Res.* **26**, 2644–2649
- Wang, Z.-Q., Stingl, L., Morrison, C., Jantsch, M., Los, M., Schulze-Osthoff, K., and Wagner, E. F. (1997) *Genes Dev.* **11**, 2347–2358
- Simbulan-Rosenthal, C. M., Rosenthal, D. S., Iyer, S., Boulares, A. H., and Smulson, M. E. (1998) *J. Biol. Chem.* **273**, 13703–13712
- Maniatis, T., Fritsch, E. F., and Sambrook, J. (1982) *Molecular Cloning: A Laboratory Manual*, Vol. 2, pp. 9.1–9.62, Cold Spring Harbor Laboratory, Cold Spring Harbor, NY
- Feinberg, A. P., and Vogelstein, B. (1983) *Anal. Biochem.* **132**, 6–13
- Bradford, M. M. (1976) *Anal. Biochem.* **72**, 248–254
- Jacobson, E. L., and Jacobson, M. K. (1997) *Methods Enzymol.* **280**, 221–230
- Aboul-El, N., Jacobson, E. L., and Jacobson, M. K. (1988) *Anal. Biochem.* **174**, 239–250
- Jacobson, M. K., Levi, V., Juarez-Salinas, H., Barton, R. A., and Jacobson, E. L. (1980) *Cancer Res.* **40**, 1797–1802
- Ndaka, N., Skidmore, C. J., and Shall, S. (1980) *Eur. J. Biochem.* **105**, 525–530
- Sims, J. L., Juarez-Salinas, H., and Jacobson, M. K. (1980) *Anal. Biochem.* **106**, 296–306
- Lin, W., Amé, J.-C., Aboul-El, N., Jacobson, E. L., and Jacobson, M. K. (1997) *J. Biol. Chem.* **272**, 11895–11901
- Jacobson, E. L., Antol, K. M., Juarez-Salinas, H., and Jacobson, M. K. (1983) *J. Biol. Chem.* **258**, 103–107
- Wielckens, K., Schmidt, A., George, E., Bredehorst, R., and Hiltz, H. (1982) *J. Biol. Chem.* **257**, 12872–12877
- Amé, J.-C., Jacobson, E. L., and Jacobson, M. K. (1998) *Mol. Cell. Biochem.*, in press
- Dantzer, F., Nasheuer, H. P., Vonesch, J. L., de Murcia, G., and Menissier-de Murcia, J. (1998) *Nucleic Acids Res.* **26**, 1891–1898
- Simbulan-Rosenthal, C. M., Rosenthal, D. S., Hiltz, H., Hickey, R., Malkas, L., Applegren, N., Wu, Y., Bers, G., and Smulson, M. E. (1996) *Biochemistry* **35**, 11622–11633
- Jacobson, E. L., Shieh, W. M., and Huang, A. C. (1998) *Mol. Cell. Biochem.*, in press
- Whitacre, C. M., Hashimoto, H., Tsai, M. L., Chatterjee, S., Berger, S. J., and Berger, N. A. (1995) *Cancer Res.* **55**, 3697–3701